Geofluids (2002) **2**, 257–271

Equations of state for basin geofluids: algorithm review and intercomparison for brines

J. J. ADAMS AND S. BACHU

Alberta Geological Survey, Edmonton, Canada

ABSTRACT

Physical properties of formation waters in sedimentary basins can vary by more than 25% for density and by one order of magnitude for viscosity. Density differences may enhance or retard flow driven by other mechanisms and can initiate buoyancy-driven flow. For a given driving force, the flow rate and injectivity depend on viscosity and permeability. Thus, variations in the density and viscosity of formation waters may have or had a significant effect on the flow pattern in a sedimentary basin, with consequences for various basin processes. Therefore, it is critical to correctly estimate water properties at formation conditions for proper representation and interpretation of present flow systems, and for numerical simulations of basin evolution, hydrocarbon migration, ore genesis, and fate of injected fluids in sedimentary basins. Algorithms published over the years to calculate water density and viscosity as a function of temperature, pressure and salinity are based on empirical fitting of laboratory-measured properties of predominantly NaCl solutions, but also field brines. A review and comparison of various algorithms are presented here, both in terms of applicability range and estimates of density and viscosity. The paucity of measured formation-water properties at *in situ* conditions hinders a definitive conclusion regarding the validity of any of these algorithms. However, the comparison indicates the versatility of the various algorithms in various ranges of conditions found in sedimentary basins. The applicability of these algorithms to the density of formation waters in the Alberta Basin is also examined using a high-quality database of 4854 water analyses. Consideration is also given to the percentage of cations that are heavier than Na in the waters.

Key words: Alberta basin, brines, density, formation water, physical properties, viscosity

Received 17 September 2001; accepted 6 May 2002

Corresponding author: S. Bachu, Alberta Geological Survey, 4th Floor, Twin Atria Building, 4999–98 Ave. NW, Edmonton, AB, Canada T6B 2X3.
E-mail: stefan.bachu@gov.ab.ca. Tel: +780 427 1517. Fax: +780 422 1459.

Geofluids (2002) **2**, 257–271

INTRODUCTION

Sedimentary basins contain many of Earth's natural resources. The formation of these resources is often a result of the migration of water, which makes up to 20% by volume of a sedimentary basin (Hanor, 1994). The flow of formation water depends in part on water physical properties, such as density and viscosity. Thus knowledge, or at least a good estimation, of these properties at *in situ* conditions is necessary to interpret past and present flow paths, hydrocarbon migration, and the formation of mineral deposits. In addition, a series of human (industrial) activities, related mostly to the containment of liquid and hazardous wastes in geological media, require proper estimation of formation water properties at *in situ* conditions. These properties are controlled by pressure and temperature, which vary in sedimentary basins from atmospheric conditions to more than 100 MPa and 300 °C, respectively, and on the type and amount of dissolved solids and gases such as CO_2 and CH_4. The salinity, or total dissolved solids (TDS), of formation waters varies over a wide range, reaching in excess of 350 000 mg L^{-1} (Hanor, 1994). Because usually the amount of dissolved gases is small, their effect on water density and viscosity is considered to be significantly smaller than the effects of salinity and temperature. Thus, the effect of dissolved gases on formation brine properties such as density and viscosity can be neglected for the range of conditions found in sedimentary basins.

The buoyancy component of the force driving (or impelling; Hubbert, 1953) the flow of formation waters enhances or retards the flow driven by other mechanisms (Bachu, 1995) and can initiate convective flow (e.g. Nield & Bejan, 1992). For a given driving force, the flow rate and injectivity depend also on viscosity (or mobility, as defined in reservoir engineering). Nevertheless, few accurate studies of the

properties of aqueous solutions have been conducted over the range of conditions found in sedimentary basins. To make predictions of water properties, these studies have relied on fitting empirical mathematical expressions either to laboratory data or to field data collected mainly by the energy industry (e.g. Correia & Kestin, 1981; Gill, 1982; Kemp *et al.*, 1989; Kestin *et al.*, 1978, 1981a, b; McCain, 1991; Phillips *et al.*, 1981; Rowe & Chou, 1970). The various studies cover different ranges of variability in these controlling parameters, thus restricting their respective applicability. This study presents a review and intercomparison of several analytical expressions commonly used to calculate the density and viscosity of basinal brines on the basis of temperature, pressure and composition. In the study, temperature is denoted by T, pressure by P and water salinity, or TDS, by S. The applicability of these expressions to Alberta Basin formation waters is also examined.

FORMATION WATER PROPERTIES

The salinity of basinal formation water varies over five orders of magnitude, from meteoric water to hypersaline brines, far exceeding seawater salinity of 35 000 mg L^{-1}. The chemical character of any water depends on the original water composition and rock mineralogy, and is the product of time-dependent processes, such as rock–water interactions and transport processes, i.e. diffusion, dispersion, mixing, and convection. Precipitation and mobilization reactions, such as albitization, dolomitization, silicate hydrolysis, thermochemical sulphate reduction and other processes, control the relative concentrations of ions in basinal waters (e.g. Hanor, 1994). Generally, chloride accounts for over 95% by mass of anions in basinal waters, with the exception of meteoric waters, which are dominated by HCO_3^- or SO_4^{-2} (Hanor, 1994). As brine salinity increases, the dominant cation is generally Na; however, in some cases, it can shift to Ca. Past halite saturation, the proportion of Mg and/or K in formation waters may also increase, while the pH can decrease to less than 4 (Hanor, 1994). Waters from basins world-wide have been subdivided into three major types. Waters with TDS lower than 10 000 mg L^{-1} usually contain major anions other than Cl^-, e.g. Na–HCO_3 or Na–SO_4 waters. The second, most prevalent water type is characterized by NaCl, but is not saturated with halite. Hyper-saline brines, with salinity greater than 300 000 mg L^{-1}, contain mostly Cl^-, and Na^+, with a varying proportion of Mg^{+2}, K^+, and Ca^{+2} (Hanor, 1994).

Given the dominance of Cl and Na ions in formation waters, most laboratory studies of physical properties used aqueous NaCl solutions as a proxy for brines at various ranges of temperatures and pressures (e.g. Kestin *et al.*, 1981a, b; Palliser & McKibbin, 1998a, b, c; Phillips *et al.*, 1981; Rowe & Chou, 1970; Zarembo & Federov, 1975). A limited number of studies have been carried out on other chloride and sulphate salt solutions (e.g. Correia & Kestin, 1981; Isono, 1984), and very few studies have considered multiple component solutions, such as seawater or brine (e.g. Gill, 1982; Kemp *et al.*, 1989). There is also a large body of literature that quantifies the effect of either temperature or pressure on saline solutions (e.g. Gates & Wood 1985), but these are not satisfactory because both parameters are needed in deep basinal settings.

In the following, some of the algorithms start from the density or viscosity of fresh water, which can be extracted from other sources (e.g. Haar *et al.*, 1984; Tremaine *et al.*, 2000). Mass fraction is defined as kg NaCl per kg solution and molality is defined as mol NaCl per kg H_2O, which can be calculated from mass fraction of NaCl by (mass fraction NaCl)/[(mass fraction of water)*(molar mass NaCl in kg mol^{-1})].

Formation water density

Seven published expressions for the density of brine or NaCl solutions are presented and compared in this study. They have been selected because of their wide use in modelling studies of basin evolution, hydrocarbon migration and accumulation, genesis of MVT mineral deposits and geothermal reservoirs (e.g. Bethke, 1985, 1986; Garven, 1985, 1989; Adenekan *et al.*, 1993; Person & Garven, 1994; Person *et al.*, 1998), and because of their applicability range. Table 1 presents a summary of the applicability ranges for pressure, temperature and salinity for these algorithms, as well as the type of fluid for which they are appropriate.

In the following, the density of pure water, dependent only on temperature and pressure, is denoted by ρ_w; water density dependent on salinity and either temperature or pressure is

Table 1 Applicability range of various algorithms for calculating brine density at various pressure, temperature and salinity conditions.

Study	Fluid	P (MPa)	T (°C)	S (mg L^{-1})‡
Rowe & Chou (1970)	NaCl solution	≤35	20–150	≤330 000
Phillips *et al*. (1981)	NaCl solution	≤50	10–350	≤260 000
Gill (1982)	seawater	≤100	≤40	≤42 000
Kemp *et al*. (1989)	electrolyte solution	≤100	≤174	≤600 000
McCain (1991)	brine	0.69–69	≤127	≤450 000
Batzle & Wang (1992)	NaCl solution	5–100	20–350	≤320 000*
Palliser & McKibbin (1998b)	NaCl solution	0.1–300	0–374.15	≤1 000 000†

*Estimate of maximum salinity determined from published graphs; †Equilibrates with solid NaCl; ‡As determined at 25 °C and 1 atm.

Table 2 Relative proportions of major ions in seawater (from Gill, 1982).

Seawater composition	Cl^-	SO_4^{-2}	Na^+	Mg^{+2}	Ca^{+2}	K^+
Mass fraction (mg g^{-1} H_2O)	19.48	2.72	10.8	1.29	0.413	0.399
Percent by mass (%)	55.07	7.72	30.62	3.68	1.17	1.10

represented by ρ_f, and saline water density, dependent on all three, by ρ_B.

Rowe & Chou (1970) developed an algorithm in CGS units for calculating the density of NaCl aqueous solutions without calculating intermediate density values. Kestin *et al.* (1981a, b) transformed the Rowe & Chou (1970) relation from CGS into SI (metric) units, and this relation is given here, although it will still be referred to as Rowe & Chou's in the following discussion because they developed it first. In the expression below P is in MPa, T is in Kelvin, and w is the mass fraction of NaCl in solution.

$$\rho_B^{-1} = A - BP - CP^2 + wD + w^2E - wFP - w^2GP - 0.5wHP^2 \quad (1)$$

The coefficients A to H are functions of temperature as follows:

$$A = 1.006741 \times 10^2 T^{-2} - 1.127522 T^{-1} + 2.84851 \times 10^{-3} - 1.5106 \times 10^{-5} T + 9.270048 \times 10^{-9} T^2$$

$$B = 1.042948 T^{-2} - 1.1933677 \times 10^{-2} T^{-1} + 5.307535 \times 10^{-5} - 1.0688768 \times 10^{-7} T + 8.492739 \times 10^{-11} T^2$$

$$C = 1.23268 \times 10^{-9} - 6.861928 \times 10^{-12} T$$

$$D = -2.5166 \times 10^{-3} + 1.11766 \times 10^{-5} T - 1.70552 \times 10^{-8} T^2$$

$$E = 2.84851 \times 10^{-3} - 1.54305 \times 10^{-5} T + 2.23982 \times 10^{-8} T^2$$

$$F = -1.5106 \times 10^{-5} + 8.4605 \times 10^{-8} T - 1.2715 \times 10^{-10} T^2$$

$$G = 2.7676 \times 10^{-5} - 1.5694 \times 10^{-7} T + 2.3102 \times 10^{-10} T^2$$

$$H = 6.4633 \times 10^{-8} - 4.1671 \times 10^{-10} T + 6.8599 \times 10^{-13} T^2$$

This expression, valid up to pressures of 35 MPa, has been used extensively in various numerical models of formation-water flow in sedimentary basins (e.g. Garven, 1985, 1989; Person & Garven, 1994; Person *et al.*, 1998).

Phillips *et al.* (1981) developed the following expression for the density of aqueous NaCl solutions based on 1300 measured data values.

$$\rho_B = -3.033405 + 10.1288163x - 8.750567x^2 + 2.663107x^3 \quad (2)$$

$$x = -9.9559e^{-0.004539 \cdot m} + 7.0845e^{-0.0001638 \cdot T} + 3.9093e^{0.00002551 \cdot P}$$

where P is pressure in bars, T is temperature in °C and m is NaCl molality (mol NaCl per kg H_2O).

This expression has been used in models of fluid flow in sedimentary basins (e.g. Bethke 1985) and geothermal systems (e.g. Adenekan *et al.*, 1993).

Gill (1982) presents an expression to calculate the density of seawater up to 40 °C and for pressures ranging from atmospheric to 100 MPa. Table 2 presents the proportions of Na^+, Ca^{+2}, Mg^{+2}, K^+, Cl^- and SO_4^{-2} (sulphate) found in seawater that were used to calculate the coefficients in this algorithm. First, the freshwater density, ρ_w, is calculated for the range of considered temperatures, and then salinity is factored in, followed by pressure.

$$\rho_w = 999.842594 + 6.793952 \times 10^{-2} T - 9.095290 \times 10^{-3} T^2 + 1.001685 \times 10^{-4} T^3 - 1.120083 \times 10^{-6} T^4 + 6.536332 \times 10^{-9} T^5 \quad (3)$$

$$\rho_f = \rho_w + S(0.824493 - 4.0899 \times 10^{-3} T + 7.6438 \times 10^{-5} T^2 - 8.2467 \times 10^{-7} T^3 + 5.3875 \times 10^{-9} T^4 + S_{12}(-5.72466 \times 10^{-3} + 1.0227 \times 10^{-4} T - 1.6546 \times 10^{-6} T^2 + S_{12} 4.8314 \times 10^{-4})) \quad (4)$$

$$\rho_B = \rho_f / (1 - P1/xkst) \quad (5)$$

where:

$S_{12} = \mathrm{sqrt}(S)$

$P1 = 0.1P$

$$xkst = K_w + S(54.6746 - 0.603459 T + 1.09987 \times 10^{-2} T^2 - 6.1670 \times 10^{-5} T^3 + S_{12}(7.944 \times 10^{-2} + 1.6483 \times 10^{-2} T - 5.3009 \times 10^{-4} T^2)) + P1(A_w + S(2.2838 \times 10^{-3} - 1.0981 \times 10^{-5} T - 1.6078 \times 10^{-6} T^2 + (S_{12})^3 1.91075 \times 10^{-4} + P1(B_w + S(-9.9348 \times 10^{-7} + 2.0816 \times 10^{-8} T + 9.1697 \times 10^{-10} T^2)))$$

$$K_w = 19652.21 + 148.4206 T - 2.327105 T^2 + 1.360477 \times 10^{-2} T^3 - 5.155288 \times 10^{-5} T^4$$

$$A_w = 3.239908 + 1.43713 \times 10^{-3} T + 1.16092 \times 10^{-4} T^2 - 5.77905 \times 10^{-7} T^3$$

$$B_w = 8.50935 \times 10^{-5} - 6.12293 \times 10^{-6} T + 5.2787 \times 10^{-8} T^2$$

Brine density (ρ_B) is in kg m^{-3}, salinity (S) is in ppt (parts per thousand or per mil), T is in °C and P is in decibars. This expression predicts higher density values than NaCl solution algorithms due to the inclusion of heavier ions, such as Ca

Table 3 Coefficients used to determine the A_{ij} component of infinite dilution molal volume (see discussion below about errors in originally published paper).

	A_{00} ($\times 10^5$)	A_{10} ($\times 10^7$)	A_{20} ($\times 10^{10}$)	A_{01} ($\times 10^7$)	A_{11} ($\times 10^{10}$)	A_{21} ($\times 10^{12}$)	A_{02} ($\times 10^{10}$)	A_{12} ($\times 10^{12}$)	A_{22} ($\times 10^{15*}$)
NaCl	−7.1929	5.6004	−8.6619	5.3789	−32.186	4.7893		2.3368	−3.9432
NaBr	−8.7988	6.6619	−9.8006	3.1588	−21.448	3.6082		1.7470	−4.8366
KCl	−6.0780	5.4133	−8.2792	0.45141			−1.5741		
KBr	−7.5382	6.5728	−9.7378	0.45141			−1.5741		
$CaCl_2$	−13.4695	9.8240	−15.783			1.2468	48.2352	−27.4651	34.3693
$CaBr_2$	−13.6982	10.5661	−16.514			1. 1752	52.5124	−29.5866	37.3999
$ZnCl_2$	1.6470								
$ZnBr_2$	−11.0575	7.5660	−10.1729		−3.0687			5.8225	

and SO_4, but its applicability to sedimentary basins is limited due the low temperature range.

Kemp *et al.* (1989) developed a model for brine density using experimental and literature data to calculate the density of NaCl, NaBr, KCl, KBr, $CaCl_2$, $CaBr_2$ and $ZnBr_2$ solutions and their mixtures. The algorithm is valid up to temperatures of 174°C (345°F) and 100 MPa, although the literature data did not cover the entire spectrum for all the components of interest. The limited data for all the salts constrain the model and its validity to the range over which the empirical parameters were fitted (Kemp *et al.*, 1989). The model is based on the apparent molal volume, υ_i, of each dissolved salt, which takes into account the short range interactions between ions and long range electrostatic interactions with other ions in the mixture. The Bronsted–Guggenheim 'specific interaction' variation of the Debye-Huckel theory is incorporated into the model to account for high ionic strength solutions. These two features make the Kemp *et al.* (1989) algorithm distinct from others presented here in that it is based on thermodynamic relationships rather than exclusive fitting to measured data.

The model starts from the density of pure water, ρ_w, known for the specified temperature T and pressure P, which is then modified for the presence of salts as follows:

$$\rho_B = (1 + \Sigma m_i M_i)/(1/\rho_w + \Sigma m_i \upsilon_i) \quad (6)$$

where ρ_B is the density of the electrolyte solution in kg m^{-3}, m_i is the molality of the ith salt, M_i is the molecular weight of the ith salt and υ_i is the apparent molal volume of the ith salt, given by:

$$\upsilon_i = \upsilon^0 + D_H + \frac{1}{2}\left(\sum_K \upsilon_K N_K B^K_{JK}\right) m_J + \frac{1}{2}\left(\sum_J \upsilon_J N_J B^J_{JK}\right) m_K \quad (7)$$

In the above relation K refers to ions of charge opposite to J, and υ_K or υ_J is the stoichiometric coefficient of K or J ions in the ith salt.

The infinite-dilution molal volume, υ°, in equation (7) can be calculated using:

$$\upsilon^0 = A_{00} + A_{01}\Delta P + A_{02}\Delta P^2 + A_{10}T + A_{11}T\Delta P + A_{12}T\Delta P^2 + A_{20}T^2 + A_{21}T^2\Delta P + A_{22}T^2\Delta P^2$$

where ΔP is the difference between *in situ* pressure and atmospheric pressure ($P - P_{atm}$) in MPa, and T is temperature in K. The coefficients A_{ij} for various salts are given in Table 3.

Also in equation (7), D_H is the Debye-Huckel term of molal volume, defined as:

$$D_H = [(A_v\sqrt{I})/2(1 + \sqrt{I})\,](\upsilon_{cation} z_{cation}{}^2 + \upsilon_{anion} z_{anion}{}^2)$$

where I is ionic strength, υ_{anion} and υ_{cation} are, respectively, the number of anions and cations in the ith salt, z_{anion} and z_{cation} are the valences of the anion and cation of the ith salt, respectively, and the Debye-Huckel Limiting Law parameter A_v is defined as:

$$A_v = 1 \times 10^{-6} e^{sum}$$

$$sum = -0.75112 + 5.6658 \times 10^{-6} T\Delta P + 1.5472 \times 10^{-5} T^2 - 4.3457 \times 10^{-8} T^2\Delta P + 3.2265 \times 10^{-11} T^2\Delta P^2.$$

The B_{JK} values in equation (7) account for interaction terms that describe relationships between ions of the salt of interest and the other ions in the solution:

$$B^M_{JK} = \sum_{i=0}^{i=2}\sum_{j=0}^{j=2} B_{ij} T^i (\Delta P)^j + B_1 f_M m_M \quad \text{and}$$

$$f_M = 0.5(\upsilon_J z_J^2 + \upsilon_K z_K^2)/\upsilon_M$$

where M = J or K.

The values B_{ij} are given in Table 4.

The coefficients N_J and N_K in equation (7) are given by:

$$N_M = z_M^2 m_M \Big/ \sum_i (z_i^2 m_i)$$

where M = J or K, and i are ions of the same charge as J or K, respectively.

It should be noted here that the originally published values for the exponents of 10, which multiply the coefficients A_{ij} and B_{ij} (Tables 3 and 4) for all salts, are 1 for A_{22} and 8 for B_{22} (Kemp *et al.*, 1989). However, these exponents do not fit the pattern of the exponents of related coefficients (see Tables 3 and 4), and the use of the A_{22} and B_{22} exponents

Table 4 Coefficients used to determine the B_{ij} component of the ion interaction terms (see discussion below about errors in originally published paper).

	B_{00} ($\times 10^6$)	B_{10} ($\times 10^9$)	B_{20} ($\times 10^{11}$)	B_{01} ($\times 10^9$)	B_{11} ($\times 10^{11}$)	B_{21} ($\times 10^{14}$)	B_{02} ($\times 10^{11}$)	B_{12} ($\times 10^{13}$)	B_{22} ($\times 10^8$)
NaCl		2.7157				7.6153		−3.5462	−9.0242
NaBr	6.6842	−34.0800	4.6652						−3.8086
KCl	9.1287	−49.3066	7.3416	−4.1250					−7.1116
KBr	11.1850	−61.8288	8.9039	−4.1250					−3.5488
$CaCl_2$	4.9949	−22.6474	3.3664	−7.1552			2.8026		−2.2953
$CaBr_2$	5.8218	−25.4804	3.6141	−7.4630			2.2843		−3.4634
$ZnCl_2$	1.9141								−1.7875
$ZnBr_2$	5.5068	−6.1731			2.7990			−1.7568	−9.2343

of 10, as published, produces values that do not fit the published density values. For example, using 10^{-8} to multiply the coefficients B_{22} in Table 4 and corresponding relations produces a number in the order of 10^{-1}, while all other products are in the order of 10^{-6}. Inspection of the example given by the authors in their Appendix A suggests that the published B_{22} value is actually the B_1 value (see Table 4, B_{22} column), which is not given explicitly anywhere in the paper. The value of the exponent for the power of 10 which multiplies the coefficient A_{22} presented here (Table 3) was chosen to be 15 by examination of the pattern of these exponents and by matching the resulting expression to calculated values reported by Kemp *et al.* (1989) within 0.2% error.

McCain (1991) presents a general function for water density based on TDS, derived on the basis of published analyses of formation waters sampled by the oil industry in various sedimentary basins. The density of saline water at 25 °C and 1 atm (Standard Temperature and Pressure, STP) is given by:

$$\rho_f = 62.368 + 0.438603S + 1.60074 \times 10^{-3}S^2 \quad (8)$$

where S is TDS in wt% and ρ_w is water density at STP in lb per cubic ft. For *in situ* conditions, ρ_f is divided by the formation volume factor, B_f, to account for the changes in volume due to the increase in pressure and temperature (compression and expansion, respectively).

$$\rho_B = \rho_f / B_f \quad (9)$$

$$B_f = (1 + \Delta V_{fP})(1 + \Delta V_{fT})$$

$$\Delta V_{fP} = -1.95301 \times 10^{-9}\, PT - 1.72834 \times 10^{-13}\, P^2T - 3.58922 \times 10^{-7}\, P - 2.25341 \times 10^{-10}\, P^2$$

$$\Delta V_{fT} = -1.0001 \times 10^{-2} + 1.33391 \times 10^{-4}\, T + 5.50654 \times 10^{-7}\, T^2$$

where T is in °F and P is in psia.

Batzle & Wang (1992) used the data of Rowe & Chou (1970), Zarembo & Fedorov (1975) and Potter & Brown (1977) to derive a different expression for brine density applicable to a wider range of temperature and pressure (Table 1) by calculating first the freshwater density at different temperature and pressure conditions according to:

$$\rho_w = 1 + 1 \times 10^{-6}(-80\,T - 3.3\,T^2 + 0.00175\,T^3 + 489\,P - 2\,TP + 0.016\,T^2P - 1.3 \times 10^{-5}\,T^3P - 0.333\,P^2 - 0.002\,TP^2) \quad (10)$$

The freshwater density can in turn be adjusted to account for dissolved solute.

$$\rho_B = \rho_w + S\{0.668 + 0.44\,S + 1 \times 10^{-6}[300\,P - 2400\,PS + T(80 + 3\,T - 3300\,S - 13P + 47PS)]\} \quad (11)$$

In the above relations, ρ_B and ρ_w are in g cm^{-3}, S is NaCl mass fraction (ppm/10^6), P is in MPa and T is in °C.

Palliser & McKibbin (1998b) used experimental and calculated data to develop correlations that closely approximate brine density for a very wide range of temperatures, pressures and solute mass fractions, using NaCl as the solute. Although approximate, the correlations are qualitatively correct and match at various phase boundaries of the solid–liquid–gas system, and also match the properties of pure water when there is no dissolved salt (Palliser & McKibbin, 1998b). This model applies from atmospheric conditions up to 3127 °C (critical point of NaCl) and pressures up to 300 MPa, making it applicable to a variety of geological systems. A companion paper (Palliser & McKibbin, 1998c) describes an expression for enthalpy, making the set of expressions useable in numerical models.

Because water in sedimentary basins commonly exists as a liquid, only the correlations for subcritical liquid NaCl solutions are presented here (Table 1). This liquid region is defined by pressures greater than the vapourization pressure and temperatures less than the critical point of water ($T_c = 374.15$ °C). Within this region, Palliser & McKibbin (1998a) define four zones:

(1) Pure water density (NaCl mass fraction: $X = 0$), which can be determined from pure water expressions (e.g. Tremaine *et al.*, 2000).

(2) Aqueous NaCl solutions with $0 < X < X_{l\_SOL}$, where X_{l_SOL} is the maximum solubility of NaCl in water at the given conditions.

(3) Aqueous NaCl solutions with $X_{l\_SOL} = X < 1$.

(4) Solid salt ($X = 1$), making the density equal to the density of NaCl.

Only zones 2 and 3 are presented here.

For the case of aqueous NaCl solutions with $0 < X < X_{l\_SOL}$, the algorithm is basically a linear interpolation between the density of a NaCl solution at 100 MPa, determined from measured data, and the density of the solution along the vaporization curve for any given temperature. In contrast, the other density algorithms presented previously are expressed as nonlinear relationships between pressure, temperature and salinity. Therefore, the Palliser & McKibbin (1998b) algorithm presented below is a simplification of the density of a NaCl solution for temperatures below 374.15 °C.

$$\rho_B(T,P,X) = \rho_{ls}(T,P_{ls}(T,X)) + [P - P_{ls}(T,X)]/[1000 - P_{ls}(T,X)] \cdot [\rho_{1000}(T,X) - \rho_{ls}(T,P_{ls}(T,X))]$$

where T is in °C, P is in bars, X is in mass fraction NaCl, and density values are in kg m^{-3}. Various intermediate density values are defined as:

$$\rho_{1000}(T, X) = \rho_w(T,P=1000) + X[1695 - \rho_w(T,P=1000)]$$

where ρ_w is the density of freshwater (e.g. equation 3, or Tremaine *et al.*, 2000).

$$\rho_{ls}(T,P) = \rho_{lw\ SAT}(T) + [\rho_{l\ SAT}(T) - \rho_{wl\ SAT}(T)] \cdot [(P_{w\ SAT}(T) - P)/(P_{w\ SAT}(T) - P_{SAT}(T))]^{1/2.2}$$

In the above relations, P_{ls} is defined as the pressure of the liquid on the surface that separates the two-phase region and the liquid region. P_{ls} can be calculated by inverting the published algorithm for X_{ls} (Palliser & McKibbin, 1998a) and assuming that X_{ls} is equal to X and P is equal P_{ls}, as follows:

$$P_{ls} = P_{w\ SAT} - (P_{w\ SAT} - P_{SAT})(X - X_{l\ SOL}(T))^{1/z}$$
where $z = 0.5\ln(10)/1.4$

$P_{w\ SAT}$ is the pressure at pure water saturation, and the related density is $\rho_{wl\ SAT}$, both of which can be determined from steam tables (e.g. Haar *et al.*, 1984). $X_{l\ SOL}$ is the maximum solubility of halite in water and can be calculated using:

$$X_{l\ SOL} = f_0 + f_1 T + f_2 T^2 + f_3 T^3$$

P_{SAT} is defined as the pressure of the fluid at saturation and is expressed as:

$$P_{SAT} = a_1 t + a_2 t^2 + a_3 t^3 + a_4 t^4 + a_5 t^5$$

where $t = (T/800)^2$

The associated density, $\rho_{l\ SAT}$ is defined as:

$$\rho_{l\ SAT} = c_0 + c_1 t + c_2 t^2 + c_3 t^3 + c_4 t^4 + c_5 t^5 + c_6 t^6$$

where $t = T/800$

$a_1 = 1.32729 \times 10^1$
$a_2 = 3.18909 \times 10^3$
$a_3 = -7.24296 \times 10^2$
$a_4 = -8.15640 \times 10^3$
$a_5 = 5.67834 \times 10^3$

$c_0 = 1.22004 \times 10^3$
$c_1 = -6.09462 \times 10^2$
$c_2 = 3.17390 \times 10^3$
$c_3 = -1.75541 \times 10^4$
$c_4 = 4.08 \times 10^4$
$c_5 = -3.73488 \times 10^4$
$c_6 = 1.18784 \times 10^4$

$f_0 = 2.635 \times 10^{-1}$
$f_1 = 7.48368 \times 10^{-6}$
$f_2 = 1.44611 \times 10^{-6}$
$f_3 = -3.80860 \times 10^{-10}$

For aqueous NaCl solutions with $X_{l\_SOL} = X < 1$, very little data have been collected and published. Palliser & McKibbin (1998b) show that $\rho_B(T,P,X_{l\_SOL}(T,P)) = \rho_{l\_SOL}(T,P)$ and suggest that $\rho_{l\_SOL}(T,P)$ is minimally dependent on pressure. Thus, $\rho_{l\_SOL}(T,P) = \rho_{l\_SOL}(T)$, which is equivalent to $\rho_{l\ SAT}$ as defined in equation 13.

Algorithm comparison

Although the Batzle & Wang (1992) algorithm has a different expression and is based on a larger data set than that of Rowe & Chou (1970), as modified by Kestin *et al.* (1981a, b), the density calculations match within <0.5% (Fig. 1), because they are based predominantly on the data set of Rowe & Chou (1970). Thus, of the two, only the Batzle & Wang algorithm will be discussed from now on.

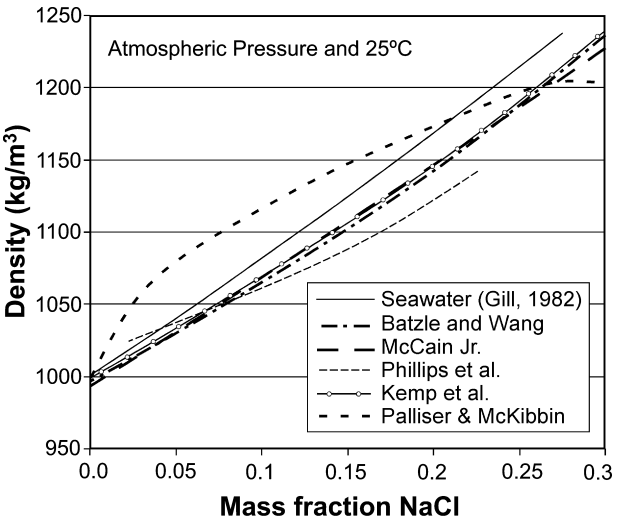

Fig. 1. Calculated brine density at standard conditions of atmospheric pressures and 25 °C, using various algorithms.

All algorithms describe, as expected, an increase in water density with increasing salinity. At STP, the Rowe & Chou (1970), McCain (1991), Kemp *et al.* (1989) and Batzle & Wang (1992) expressions all predict similar density values over a wide range of salinity (Fig. 1). The Kemp *et al.* (1989) algorithm produces density values very close to that of McCain (1991) and Batzle & Wang (1992) for salinity values up to 26 wt% NaCl, beyond which it predicts higher density with a trend of going out of range (Fig. 1). The Phillips *et al.* (1981) algorithm produces significantly different density values from the others, i.e. markedly lower density for high salinity waters (Fig. 1). The Gill (1982) expression, although used out of its valid range, estimates the highest density values because of the inclusion of higher molecular-weight ions contained in seawater, e.g. Mg, Ca, SO_4, and K, in addition to Na^+ and Cl^-. Compared to other solutions, the Palliser & McKibbin (1998a, b, c) algorithms greatly overestimate the density up to the saturation point (approximately 26 wt% NaCl), after which they underestimate it. All expressions, with the exception of that of Phillips *et al.* (1981) predict very closely the density of freshwater at 25 °C ($\rho_0 = 997.07\,kg\,m^{-3}$), i.e. Rowe & Chou (1970): $\rho_0 = 997.135$; Batzle & Wang (1992): $\rho_0 = 996.077$; Gill (1982): $\rho_0 = 997.169$; Phillips *et al.* (1981): $\rho_0 = 1012.86$; Kemp *et al.* (1989) and Palliser & McKibbin (1998a, b, c): $\rho_0 = 997.07$ by definition of the freshwater density algorithm, and McCain (1991): $\rho_0 = 995.135$. Over a range of 0–30 wt% NaCl, water density increases more than $200\,kg\,m^{-3}$, or approximately 20% of freshwater density at STP.

In the subsurface, elevated temperatures reduce brine density, whereas higher pressures increase density. Figure 2 shows predicted brine density values for temperature and pressure conditions usually found in sedimentary basins at shallow-to-intermediate, intermediate and large depths. The McCain (1991), Kemp *et al.* (1989) and Batzle & Wang (1992) algorithms predict very similar density values, into intermediate depth conditions, with differences <1% (Figs 1 and 2). The Kemp *et al.* (1989) algorithm predicts values very close to those of McCain (1991) and Batzle & Wang (1992), with somehow larger differences for large depth and salinity conditions. The Phillips *et al.* (1981) expression consistently predicts higher density at low salinity, and significantly lower density for high salinity. The Gill (1982) expression cannot estimate formation water density under most sedimentary basin conditions. The consistent and significant underestimation of density for high salinity and the lack of fit with freshwater density by the Phillips *et al.* (1981) expression suggest that this algorithm should not be used. Lacking an independent set of data for comparison, it is not possible to select definitively between the McCain (1991), Kemp *et al.* (1989) and Batzle & Wang (1992) expressions. However, the Kemp *et al.* (1989) algorithm is significantly more complex and requires an independent formulation for the density of freshwater and a detailed knowledge of the ionic composition of formation water, hence it is less suitable for use in numerical simulations of nonreactive fluid flow. The McCain (1991) algorithm is based on analyses of formation waters produced in oil fields, while the Batzle & Wang (1992) algorithm is based on NaCl aqueous solutions. On the other hand, the Batzle & Wang (1992) algorithm covers a wider range of temperature and pressure than the McCain (1991) algorithm, hence it may be more versatile for studies within sedimentary basins.

Correcting measured density for formation conditions

Determinations of formation water density are usually performed at laboratory conditions (STP) on water samples

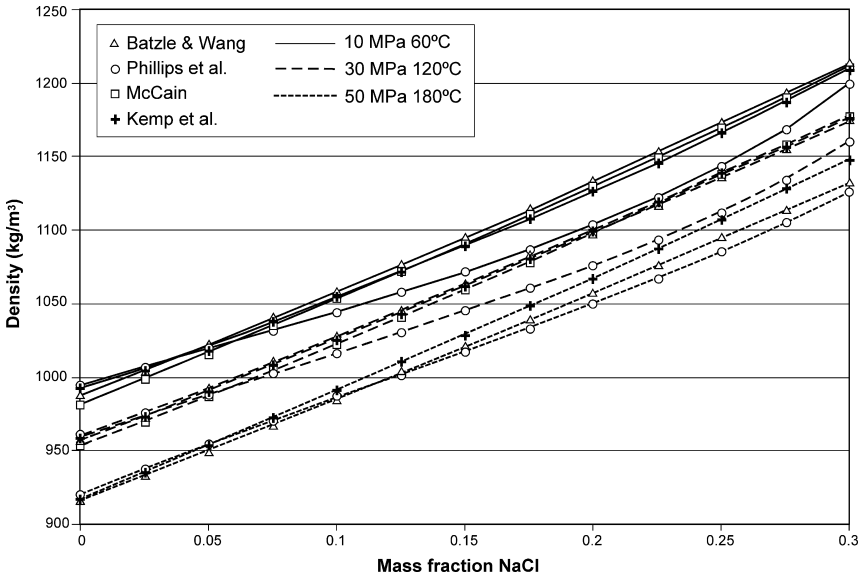

Fig. 2. Calculated brine density at various conditions characteristic of sedimentary basins.

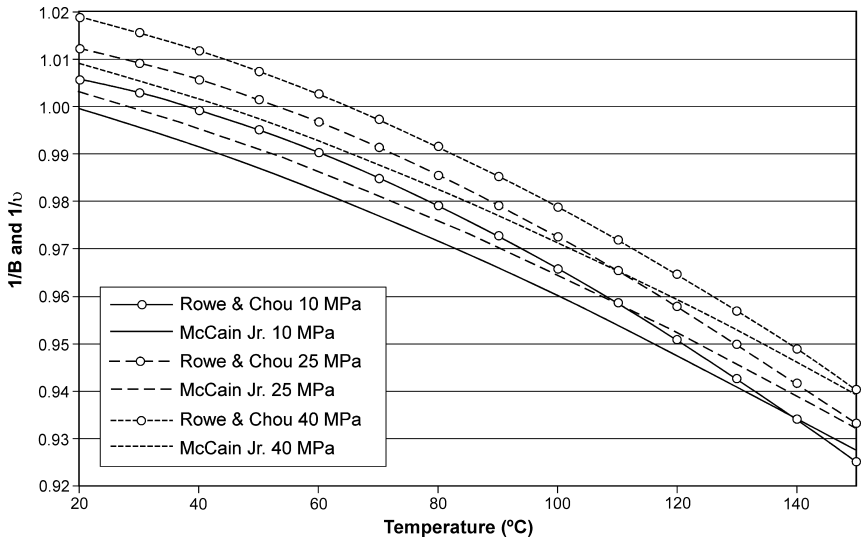

Fig. 3. Comparison of Rowe & Chou (1970) and McCain (1991) factors for adjusting formation water density at atmospheric conditions to *in situ* conditions, as functions of temperature and pressure.

collected in the energy industry, for which case predictions of density values at *in situ* conditions may be necessary. If the salinity is known and if the solutes are predominantly NaCl, then one of the previously discussed algorithms can be applied to estimate formation water density. However, in many cases the salinity is not necessarily known, or there are other ions present in the water in sufficient quantities to make unfit estimates based on NaCl solutions.

The McCain (1991) algorithm can be used to correct the water density measured at STP for pressure and temperature effects using the formation volume factor B_f [equation (9) and Table 1]. Rowe & Chou (1970) present the following expression, based on International Steam Tables, for the specific volume, υ ($cm^3\,g^{-1}$), of freshwater, as a function of temperature T (K) and pressure P ($kgf\,cm^{-2}$):

$$\upsilon_0 = A(T) - PB(T) - P^2C(T) \tag{12}$$

$$A(T) = 5.916365 - 0.01035794T + 0.9270048 \times 10^{-5}\,T^2 - 1127.522/T + 100674.1/T^2$$

$$B(T) = 0.5204914 \times 10^{-2} - 0.10482101 \times 10^{-4} \cdot T + 0.8328532 \times 10^{-8}T^2 - 1.1702939/T + 102.2783/T^2$$

$$C(T) = 0.118547 \times 10^{-7} - 0.6599143 \times 10^{-10}T$$

Equation (12) is valid for $30\,^{\circ}C \le T \le 180\,^{\circ}C$ and $P \le 40$ MPa, and can be used for scaling the salinity-dependent density measured at STP, ρ_m, to formation conditions, according to:

$$\rho_B = \rho_m/(\rho_0\upsilon_0) \tag{13}$$

where $\rho_0 = 1\,g\,cm^{-3}$. The term $\rho_0\upsilon_0$, being dimensionless, means that ρ_B has the same units as ρ_m. Application of this correction implicitly assumes that the temperature and pressure effects on brine density are independent of the presence of dissolved solids (salinity), as does the equation of McCain (1991) [equation (9)]

Figure 3 compares the factors for adjusting formation water density at STP to *in situ* conditions according to equations (9) (McCain, 1991) and (13), respectively. Both relations show the expected dependence of density on temperature and pressure; although equation (13) predicts slightly higher density values than McCain (1991), by up to 0.6%.

Formation water viscosity

Water or brine viscosity is strongly dependent on temperature (decreases with increasing temperature), less dependent on salinity, and almost negligibly dependent on pressures (increases with increasing salinity or pressure). Four published algorithms for calculating brine viscosity are presented, with the corresponding applicability ranges shown in Table 5. Some of them neglect the viscosity dependence on pressure. In the following, brine viscosity is denoted by μ_B, and an intermediate water viscosity dependent on temperature and/or salinity and/or pressure, but not all three, is represented by μ_w.

Mercer *et al.* (1975) present the following expression for water viscosity as a function of temperature only:

$$\mu_w = [(5.38 + 3.80\,A - 0.26A^3)10^3]^{-1} \tag{14}$$

$$A = 0.01(T - 150)$$

where T is temperature in °C, and μ_w is in Pa · s. This expression is included here for comparison only.

Kestin *et al.* (1981a, b) developed the following algorithm for calculating the viscosity of NaCl aqueous solutions:

$$\mu_B = \mu(1 + \beta P) \tag{15}$$

where

$$\mathrm{Log}(\mu) = A + 3.000867722 + C(B + 1)$$

Table 5 Applicability range of various algorithms for calculating brine viscosity at various temperature, salinity and pressure conditions.

Study	Fluid	T (°C)	S (mg L^{-1})	P (MPa)
Kestin *et al*. (1981a, b)	NaCl solution	20–150	≤460 000	0.1–35
Phillips *et al*. (1981)	NaCl solution	10–350	≤420 000	–
McCain (1991) –1	brine	30–200	≤350 000	–
McCain (1991) –2	brine	30–75	≤350 000	≤100
Batzle & Wang (1992)	NaCl solution	≤250	≤460 000	–
Palliser & McKibbin (1998c)	NaCl solution	<800	≤1000 000	0.1–300

$$A_1 = 3.324 \times 10^{-2} \quad B_1 = -3.96 \times 10^{-2}$$
$$A_2 = 3.624 \times 10^{-3} \quad B_2 = 1.02 \times 10^{-2}$$
$$A_3 = -1.879 \times 10^{-4} \quad B_3 = -7.02 \times 10^{-4}$$

$$A = A_1 S + A_2 S^2 + A_3 S^3$$
$$B = B_1 S + B_2 S^2 + B_3 S^3$$
$$C = 1.2378(20 - T) - 1.303 \times 10^{-3}(20 - T)^2 + 3.06 \times 10^{-6}(20 - T)^3 + 2.55 \times 10^{-8}(20 - T)^4/(96 + T)$$
$$\beta = \beta_s \cdot \beta_p + \beta_w$$
$$\beta_w = -1.297 + 5.74 \times 10^{-2}\, T - 6.97 \times 10^{-4}\, T^2 + 4.47 \times 10^{-6}\, T^3 - 1.05 \times 10^{-8}\, T^4$$
$$\beta_s = 0.545 + 2.8 \times 10^{-3}\, T - \beta_w$$
$$\beta_p = 2.5(S/m_s) - 2(S/m_s)^2 + 0.5(S/m_s)^3$$
$$m_s = 6.044 + 2.8 \times 10^{-3}\, T + 3.6 \times 10^{-5}\, T^2$$

where P is pressure in MPa, T is in °C, S is the mass fraction of NaCl in the NaCl solution and μ_B is in Pa · s. This algorithm has been used in various models of flow in sedimentary basins (e.g. Garven, 1985, 1989; Person & Garven, 1994).

Phillips *et al.* (1981) developed the following expression for the viscosity (in cP) of NaCl aqueous solutions as a function of temperature T (°C) and NaCl molality, m, based on work carried out by Vand (1948):

$$\mu_B = \mu_w [1 + 0.0816\, m - 0.0122\, m^2 + 0.000128\, m^3 + 0.000629\, T(1 - e^{-0.7m})] \quad (16)$$

where μ_w is the viscosity of freshwater at the corresponding temperature. Phillips *et al.* (1981) use for μ_w a correlation published by Watson *et al.* (1980), but others are using various other expressions available in the literature, including steam tables (Haar *et al.*, 1984). Although pressure is not explicitly included in this correlation, the data are considered accurate for pressures up to 50 MPa. This formulation has been used to correct for salinity effects in models of flow in geothermal reservoirs (e.g. Battistelli *et al.*, 1997) and of variable-density fluid flow in sedimentary basins (e.g. Bethke, 1985, 1986).

McCain (1991) presents the following general function for saline water viscosity that depends only on salinity (TDS) and temperature (referred to in Table 5 as McCain-1):

$$\mu_B(T) = A\, T^{-B} \quad (17)$$

$$A = 109.574 - 8.40564\, S + 0.313314\, S^2 + 8.72213 \times 10^{-3}\, S^3$$
$$B = 1.12166 - 2.63951 \times 10^{-2}\, S + 6.79461 \times 10^{-3}\, S^2 + 5.47119 \times 10^{-5}\, S^3 - 1.55586 \times 10^{-6}\, S^4$$

where T is in °F, S is in wt% and μ_w is in centipoises (cP).

For nonatmospheric pressure conditions, McCain (1991) proposes an adjustment (McCain-2 in Table 5); however, the following relationship has a limited temperature range of applicability (Table 5):

$$\mu_B(T,P) = \mu_B(T)(0.9994 + 4.0295 \times 10^{-5}\, P + 3.1062 \times 10^{-9}\, P^2) \quad (18)$$

where P is in psia.

Batzle & Wang (1992) used the curves in Matthews & Russel (1967) to extend the relationship for the viscosity of NaCl aqueous solutions developed by Kestin *et al.* (1981a, b; Table 5). They deemed the effect of pressure as negligible and therefore did not consider it in the following expression. Viscosity at different temperature and salinity conditions is defined as:

$$\mu_B = 0.1 + 0.333\,(S + (1.65 + 91.9)S^3)e^{-A} \quad (19)$$
$$A = (0.42(S^{0.8} - 0.17)^2 + 0.045)T^{0.8}$$

where μ_B is in cP, S is the NaCl mass fraction (ppm/10^6), and T is in °C.

Palliser & McKibbin (1998c) used experimental and calculated data to develop approximate, but qualitatively correct correlations that closely describe brine enthalpy and viscosity for the same range of temperatures, pressure and solute mass fractions as for density (Palliser & McKibbin, 1998b). They chose the viscosity algorithm of Phillips *et al.* (1981) as a basis for their extrapolation to higher temperatures and pressures. For temperatures less than 800 °C, the viscosity correlation is:

$$\mu_B(T,P,X) = \frac{\left\{\begin{array}{c}\mu_w(T,P)[1 + 3X][(800 - T)/800]^9 \\ +(T/800)^9[\mu_w(T,P)(1 - X) + \mu_c(800)X]\end{array}\right\}}{\left[\frac{800 - T}{800}\right]^9 + \left(\frac{T}{800}\right)^9}$$

where X is the dissolved NaCl concentration in mass fraction, T is in °C and $\mu_w(T,P)$ is the viscosity of pure water at *in situ*

conditions; $\mu_c(800)$ is the viscosity of liquid NaCl at 800°C, calculated as follows:

$$\mu_c(800) = 4.71624 \times 10^{-3} - 4.02030 \times 10^{-6} 800.$$

At low temperatures (approximately 50 °C), Phillips *et al.* (1981) viscosity algorithm is visibly nonlinear with respect to salinity; however, the above μ_B equation appears almost linear. The difference between the Phillips *et al.* (1981) and Palliser & McKibbin (1998c) algorithms diminishes as temperature increases.

Algorithm comparison

Not all these viscosity algorithms are dependent on pressure, temperature and salinity effects, and therefore they are compared first for atmospheric pressure conditions. The expression given by Weast (1988), based on the National Institute of Standards, was used for the freshwater viscosity μ_w needed in equation (16) instead of the original one used by Phillips *et al.* (1981). Viscosity in general is most sensitive to temperature. In the case of water, an increase in temperature results in a decrease in viscosity by one order of magnitude and more from freshwater viscosity at STP (Fig. 4).

Basically, for low salinity waters, all the algorithms, including the Mercer *et al.* (1975) relation, which depends only on temperature, provide similar estimates of water viscosity (Fig. 4). The expression of Batzle & Wang (1992) produces higher viscosity values than the other solutions, by up to 10%, for $T < 120$ °C. The differences are most probably due to different curve-fitting procedures used by the various authors. Increases in salinity have the opposite effect on water viscosity to temperature, but to a much lesser degree. Viscosity increases only by a factor of less than 3 as a result of salinity increases (Fig. 5). The Kestin *et al.* (1981a, b) and Phillips *et al.* (1981) expressions predict almost identical viscosity values, consistently lower than all the others, with an increasingly significant difference as salinity increases. The Palliser & McKibbin (1998c) algorithm has a quasi-linear behaviour of increasing viscosity with salinity, and, for low temperatures, predicts viscosity values higher by up to 10% than the other two for salinity values up to 0.19 mass fraction, after which it predicts increasingly lower viscosity (Fig. 5). The algorithm of McCain (1991) predicts viscosity values close to those of Kestin *et al.* (1981a, b) and Phillips *et al.* (1981) for salinity values up to 25 wt% NaCl. The algorithm of Batzle & Wang (1992) predicts higher values, by up to 15%, than those of Kestin *et al.* (1981a, b) and Phillips *et al.* (1981) for salinity <25 wt% NaCl (Fig. 5). Prediction of higher viscosity values at high temperatures by the McCain (1991) algorithm is most likely due to the fact that the former is based on brines, which contain a large proportion of heavier ions than the NaCl solution used by Kestin *et al.* (1981a). The effect of heavier ions on brine viscosity is demonstrated by the slightly higher viscosity of $CaCl_2$ aqueous solutions (Isono 1984), shown for comparison in Fig. 5.

The effect of pressure on viscosity, although directionally similar to that of salinity, is very small (e.g. Phillips *et al.* 1981). Generally, the effect of pressure causes a <5% increase in brine viscosity over the range of pressures encountered in sedimentary basins. Figure 6 compares viscosity predictions for various pressures characteristic of sedimentary basins. Both of the algoritmes of McCain (1991), with and without pressure effect, are presented (McCain – 1 and McCain – 2, respectively). The effect of pressure on viscosity is very small in the case of the Kestin *et al.* (1981a, b) and Palliser & McKibbin (1998c) algorithms (Fig. 6). The viscosity predicted by the 'no-pressure' McCain (1991) algorithm is very

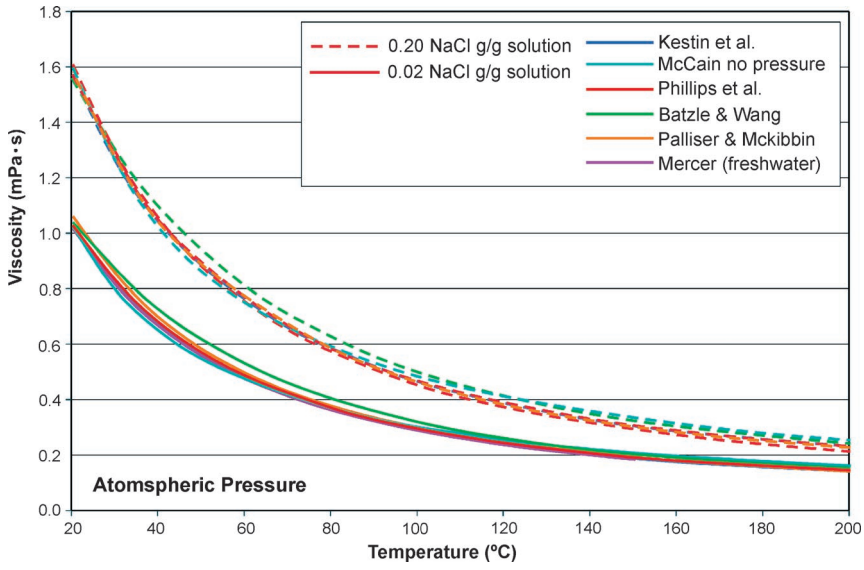

Fig. 4. Dependence on temperature of viscosity for low and high salinity waters at atmospheric pressure.

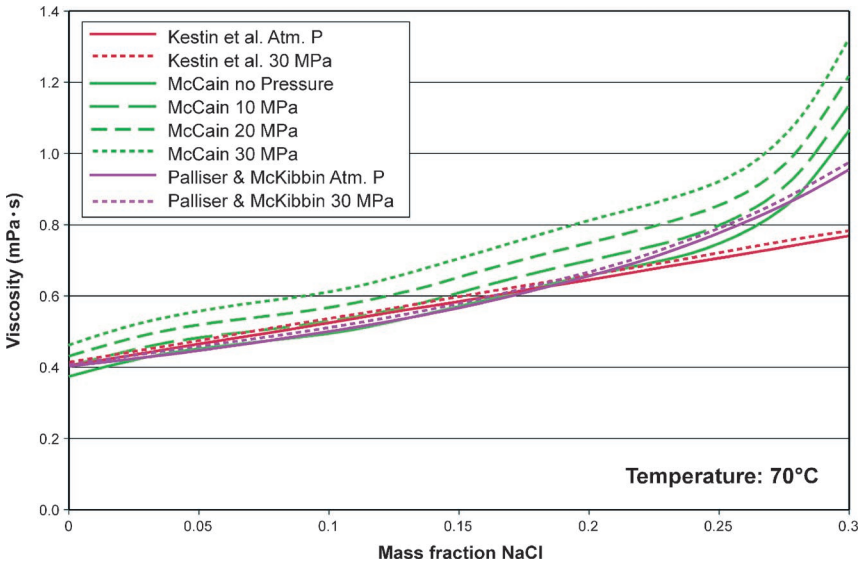

Fig. 5. Dependence on salinity of viscosity for low and high temperature waters at 10 MPa.

close to Kestin *et al.* (1981a, b) values for salinity <12 wt% NaCl. However, the viscosity predicted by McCain's pressure-corrected expression (McCain 1991) is significantly greater (by up to 50%) than that predicted by the Kestin *et al.* (1981a, b) algorithm. This behaviour is inconsistent with the understanding of the minimal impact pressure has on viscosity.

The pressure-corrected algorithm presented by McCain (1991) has limited applicability for brines in sedimentary basins ($T \leq 75$ °C) and seems to grossly over-correct (over-estimate) for pressure effects, while the uncorrected one is limited to salinity <25 wt% NaCl. The Phillips *et al.* (1981) algorithm and that presented by Kestin *et al.* (1981a, b) produce almost identical viscosity values for any set of conditions. Due to the lack of measured field data, it is difficult to conclusively select a preferred algorithm for calculating brine viscosity. Only the Kestin *et al.* (1981a, b) and Palliser & McKibbin (1998c) algorithms account for temperature, salinity and pressure over the range of basin conditions. However, the Palliser & McKibbin (1998c)

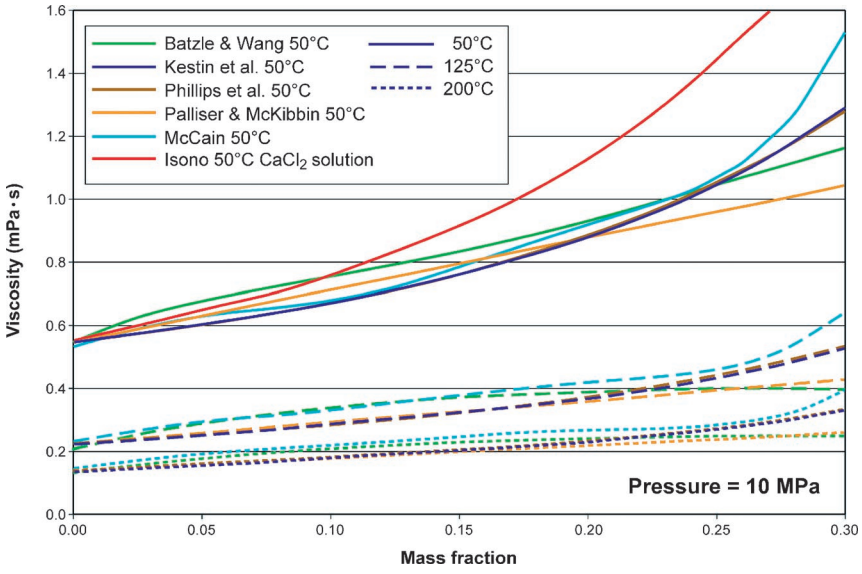

Fig. 6. Effect of pressure on formation water viscosity at 70 °C, as predicted by the Kestin *et al.* (1981a, b), McCain (1991) and Palliser & McKibbin (1998c) algorithms.

algorithm seems to increasingly underpredict brine viscosity for salinity greater than 19 wt% NaCl. On the other hand, only the McCain (1991) algorithm is based on brine data from sedimentary basins, rather than NaCl aqueous solutions, and the presence of heavier ions seems to compensate for the lack of pressure effects. The differences between these three algorithms are small, and certainly smaller than the errors introduced into calculations by all the errors in measurement and estimates of formation water salinity, pressure and temperature. Lacking data, the viscosity of low salinity waters at relatively low pressures ($< 50\,000$ mg L^{-1} and <20 MPa, respectively), can be accurately predicted by the Mercer *et al.* (1975) expression, if at least temperature is known.

DENSITY OF FORMATION WATER IN THE ALBERTA BASIN

The salinity of formation waters in the Alberta Basin, which is located in western Canada east of the Rocky Mountains, varies from freshwater (<1000 mg L^{-1} TDS) to in excess of 27 eqv. wt% NaCl (350 000 mg L^{-1} TDS). The brines are dominantly Na–Cl waters, but they also contain dissolved metals, such as Mg^{2+}, Ca^{+2} and Li^{+}. There are no specific studies to date that have measured the density of Alberta Basin waters at the temperature and pressure conditions that occur in the basin (up to 200°C and approximately 70 MPa, respectively).

As a result of requirements by provincial regulatory agencies, a database of more than 185 000 standard analyses of formation water samples collected by the energy industry, of extremely variable quality, is available in the public domain. These analyses have been culled based on some 24 different criteria using automatic and manual methods (Hitchon & Brulotte, 1994; Hitchon, 1996), to eliminate incomplete, erroneous and/or contaminated analyses. Analyses that did not report Na^{+} or TDS, or that report out-of-range density values at atmospheric conditions (<1000 kg m^{-3} or >1300 kg m^{-3}) were also eliminated. Analyses that report $K/Na > 0.5$ were culled because such high ratios are suspect in the Alberta Basin where KCl salts are absent (Hitchon & Brulotte, 1994; Hitchon, 1996). Samples with a difference greater than 5% between the measured TDS and the sum of all major ions were eliminated. Finally, analyses were checked for charge balance according to:

$$\text{Charge balance} = 2(\Sigma \text{ cations} - \Sigma \text{ anions})/(\Sigma \text{ cations} + \Sigma \text{ anions}). \quad (20)$$

Only analyses with a charge balance <5% were retained. The following ions were used in the balance and TDS calculations: Cl^{-}, HCO_3^{-}, CO_3^{-2}, SO_4^{-2}, Mg^{+2}, Ca^{+2}, Na^{+} and K^{+}.

The result is a database of approximately 24 000 high-quality analyses of formation waters, of which less than half report density measurements at STP conditions, in addition to the major ions. Of these, only the samples that report both K^{+} and Na^{+} were retained, because this is an indicator of extensive analysis, the inference being that the quality is higher. This quality checking process resulted in a superior data set of 4854 formation water analyses that report density measurements.

The data generally follow a distinct linear trend of increasing density with salinity (Fig. 7). Density values calculated using both the McCain (1991) and Batzle & Wang (1992) algorithms (equations 1 & 2, and 4 & 5, respectively) are generally lower than the corresponding measured values,

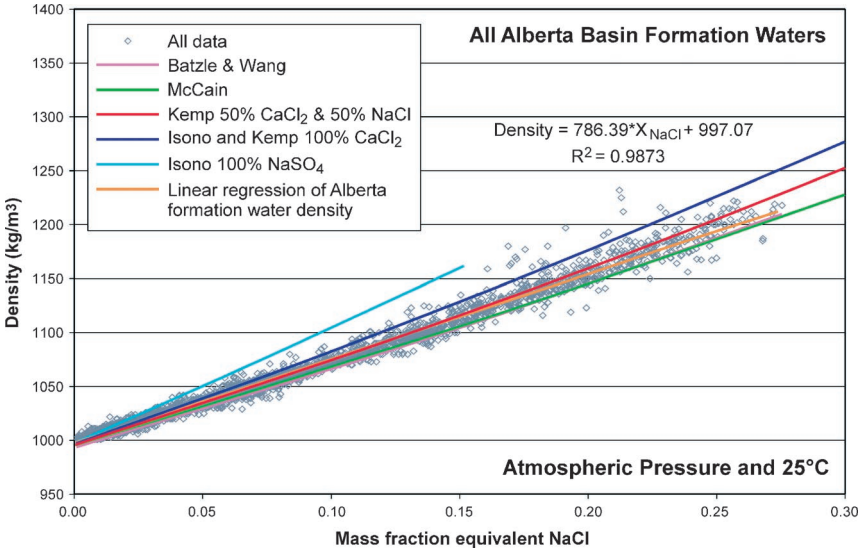

Fig. 7. Variation of measured density at atmospheric conditions with salinity for formation waters in the Alberta Basin. Density values for NaCl solutions predicted by the Kemp *et al.* (1989), McCain (1991) and Batzle & Wang (1992) algorithms are also shown (indistinguishable one from another), together with a simple linear-regression fit. Measured density values for $NaSO_4$ solutions and $CaCl_2$ solutions (Isono 1984) are plotted for comparison. Salinity of formation waters is reported in mg L^{-1} from laboratory analyses. These salinity values were converted to mass fraction by dividing the salinity by the reported density and converting the units.

with increasingly significant differences as the salinity increases (Fig. 7). The density of low salinity brines (TDS < 5 eqv. wt% NaCl) can be reasonably estimated using either the Batzle & Wang (1992) or McCain (1991) algorithm.

The abundance of Ca^{2+}, Mg^{2+} and $SO_4{}^{2-}$ in some of the Alberta Basin formation waters, particularly in Palaeozoic strata, suggests that a correction for these ions as $CaCl_2$, $MgCl_2$ and Na- or Ca-SO_4 needs to be made in calculating brine density. Sulphate species have high molecular weights, starting at 118 g mol^{-1}, compared to the molecular weights of 58 g mol^{-1} for NaCl, 110 g mol^{-1} for $CaCl_2$ or 83 g mol^{-1} for $NaHCO_3$, with corresponding effects on brine density (see Isono, 1984) measurements for SO_4 (Fig. 7). Thus, small mass fractions of Ca and/or SO_4 in formation water may significantly affect brine density. Using the Kemp *et al.* (1989) algorithm with increasing $CaCl_2$ content (up to 50%) produces a better fit with the data (Fig. 7). Introducing heavier ions as salinity increases, will probably increase the accuracy of the fit.

As an alternative solution, the STP density of brines in the Alberta Basin can be estimated by using a linear regression derived from the measured data. For pure water the regression should retrieve the density of freshwater at STP ($\rho_f = 997.07$ kg m^{-3}). Thus, the regression line was fit to pass through this value (Fig. 7), resulting in a very good fit ($R^2 = 0.9873$). Because this regression line is fitted to data at STP, either the Rowe & Chou (1970) or McCain (1991) algorithm (equations 11 or 2, respectively) can be applied to the predicted water density at STP conditions, to bring it to formation temperature and pressure conditions.

DISCUSSION AND CONCLUSIONS

Physical properties of formation waters in sedimentary basins can vary by more than 25% for density and by one order of magnitude for viscosity, relative to freshwater at standard conditions, as a result of variations in salinity, temperature and pressure. Density and viscosity increase with increasing salinity and pressure, whereas increasing temperature causes a decrease in density and viscosity. Over the range of conditions encountered in a basin, salinity may have the greatest impact on density, followed by temperature. Viscosity is most sensitive to temperature and less so to salinity. For both density and viscosity, pressure causes the least variation due to the low compressibility of water.

The effects of salinity, temperature and pressure on formation water density and viscosity need to be taken into account when assessing the flow of basinal fluids because complete neglect of density and viscosity variations introduces significant errors in assessing both flow strength and direction (Bachu 1995). Several algorithms have been published over the years to calculate water density and viscosity as a function of temperature, pressure and salinity. These algorithms are based on empirically fitting of laboratory-measured properties of predominantly NaCl solutions, but also field brines. The algorithms are variously used in numerical models of basin evolution, hydrocarbon migration, mineral deposition, geothermal reservoirs and fluid injection. A comparison of these algorithms, both in terms of applicability range and estimates, shows that the difference between density estimates by various algorithms increases with salinity, reaching up to 20% for 40 eqv. wt% NaCl. For viscosity, these differences may reach 50% when both salinity and pressure effects are taken into account.

Considering that rock permeability varies within several orders of magnitude, the differences introduced by various methods in assessing water density and viscosity are most likely negligible in comparison with the errors and uncertainty introduced by estimating rock properties, especially permeability, on the basis of small-scale and/or sparse measurements. This is particularly true for low-salinity water, in regional- and basin-scale studies of formation water flow and transport, where forces other than buoyancy are dominant. Nevertheless, there are situations when these differences may have a significant impact, in which case the proper estimation of water density and viscosity becomes critical. For example, when the magnitude of buoyancy is comparable with other flow-driving forces and differences in evaluating water density may significantly affect the estimated magnitude and direction of the flow-driving force (Bachu & Michael, 2002), particularly for high-salinity brines commonly found in many North American mid-continent basins. Similarly, estimates in flow strength may be off by one order of magnitude as a result of differences in calculating brine viscosity. Multiphase fluid flow is another case for which the proper estimation of water density and viscosity is critical. For instance, estimation of the fate of formation water and another fluid, such as supercritical CO_2, must take into account gravity override and viscous fingering.

The paucity of measured formation-water properties at *in situ* conditions hinders any definitive conclusion regarding the validity of each examined algorithm. However, the comparison indicates that, for formation water density, the McCain (1991) and Batzle & Wang (1992) algorithms seem to be the most versatile. These expressions predict very similar values for the range of conditions found in sedimentary basins and can be easily used in numerical models. The Batzle & Wang (1992) algorithm is accurate over a wider range of conditions than that of McCain (1991), and therefore should be preferred. For viscosity, the Kestin *et al.* (1981a, b) algorithm seems to be the most versatile for basin conditions.

For low salinity (<5 eqv. wt% NaCl), STP-measured Alberta Basin brine density is well predicted by both the McCain (1991) and Batzle & Wang (1992) algorithms; however, for higher salinity these algorithms increasingly under-

estimate brine density, reaching a difference of 40 kg m^{-3} for 25 wt% NaCl (300 000 mg L^{-1}) salinity. The cause of this deviation is most likely the high content of heavy ions in these brines, particularly Ca. The density of formation waters in the Alberta Basin can be well described empirically by a linear regression of density as a function of salinity. These density estimates can then be adjusted to formation temperature and pressure using available algorithms, such as those of Rowe & Chou (1970) or McCain (1991).

Because density and viscosity variations significantly affect patterns of formation water flow in a sedimentary basin, the present analysis provides a tool for the proper estimation of these formation-water properties at *in situ* conditions.

REFERENCES

Adenekan A, Patzek ETW, Preuss K (1993) Modeling of multiphase transport of multicomponent organic contaminants and heat in the subsurface. *Water Resources Research*, **29**, 3727–40.

Bachu S (1995) Flow of variable-density formation water in deep sloping aquifers: review of methods of representation with case studies. *Journal of Hydrology*, **164**, 19–38.

Bachu S, Michael K (2002) Flow of variable-density water in deep sloping aquifers: minimizing the error in representation and analysis when using hydraulic-head distributions. *Journal of Hydrology*, **259**, 49–65.

Battistelli A, Calore C, Preuss K (1997) The simulator TOUGH2/EWASG for modeling geothermal reservoirs with brines and non-condensible gas. *Geothermics*, **26**, 437–64.

Batzle M, Wang Z (1992) Seismic properties of pore fluids. *Geophysics*, **57**, 1396–1408.

Bethke CM (1985) A numerical model of compaction-driven groundwater flow and heat transfer and its application to the paleohydrology of intracratonic sedimentary basins. *Journal of Geophysical Research*, **90**, 6817–28.

Bethke CM (1986) Hydrologic constraints on genesis of the Upper Mississippi Valley Mineral District from Illinois Basin brines. *Economic Geology*, **81**, 233–49.

Correia RJ, Kestin J (1981) Viscosity and density of aqueous Na_2SO_4 and K_2SO_4 solutions in the temperature range 20–90 °C and pressure range 0–30 MPa. *Journal of Chemical Engineering Data*, **26**, 43–7.

Garven G (1985) The role of regional fluid flow in the genesis of Pine Point deposit, Western Canada Sedimentary Basin. *Economic Geology*, **80**, 307–24.

Garven G (1989) A hydrogeologic model for the formation of the giant oil sands deposits of the Western Canada Sedimentary Basin. *American Journal of Science*, **289**, 105–66.

Gates JA, Wood RH (1985) Densities of aqueous solutions of NaCl, $MgCl_2$, KCl, NaBr, LiCl and $CaCl_2$ from 0.05 to 5.0 mol kg^{-1} and 0.1013–40 MPa at 298.15 K. *Journal of Chemical Engineering Data*, **30**, 44–9.

Gill AE (1982) *Atmosphere-Ocean Dynamics*. Academic Press, New York.

Haar L, Gallagher JS, Kell GS (1984) *NBS/NRC Steam Tables*. Hemisphere Publishing Co, Washington, DC.

Hanor JS (1994) Origin of saline fluids in sedimentary basins. In: Geofluids: Origin, Migration and Evolution of Fluids in Sedimentary Basins (ed J. Parnell), *Geological Society of London Special Publication*, **78**, 151–74.

Hitchon B (1996) Rapid evaluation of the hydrochemistry of a sedimentary basin using only 'standard' formation water analyses: example from the Canadian portion of the Williston basin. *Applied Geochemistry*, **11**, 789–95.

Hitchon B, Brulotte M (1994) Culling criteria for 'standard' formation water analyses. *Applied Geochemistry*, **9**, 637–45.

Hubbert K (1953) Entrapment of petroleum under hydrodynamic conditions. *Bulletin of American Association of Petroleum Geologists*, **37**, 1954–2026.

Isono T (1984) Density, viscosity and electrolytic conductivity of concentrated aqueous electrolyte solutions at several temperatures. Alkaline-Earth Chlorides, $LaCl_3$, Na_2SO_4, $NaNO_3$, NaBr, KNO_3, KBr, and Cd $(NO_3)_2$. *Journal of Chemical Engineering Data*, **29**, 45–52.

Kemp NP, Thomas DC, Atkinson G, Atkinson BL (1989) Density modeling for brines as a function of composition, temperature and pressure. *SPE Production Engineering*, **4**, 394–400.

Kestin J, Khalifa HE, Abe Y, Grimes CE, Sookiazian H, Wakeham WA (1978) Effect of pressure on viscosity of Aqueous NaCl solutions in the temperature range 20–150 °C. *Journal of Chemical and Engineering Data*, **23**, 328–36.

Kestin J, Khalifa HE, Correia RJ (1981a) Tables of dynamic and kinematic viscosity of aqueous KCl solutions in the temperature range 25–150 °C and the pressure range 0.1–35 MPa. *Journal of Physical Chemistry Reference Data*, **10**, 57–70.

Kestin J, Khalifa HE, Correia RJ (1981b) Tables of dynamic and kinematic viscosity of aqueous KCl solutions in the temperature range 25–150 °C and the pressure range 0.1–35 MPa. *Journal of Physical Chemistry Reference Data*, **10**, 71–87.

Matthews CS, Russel DG (1967) *Pressure Buildup and Flow Test in Wells*. Monograph **Vol. 1**. H.L Doherty Series; Society of Petroleum Engineering of AIME.

McCain WD Jr (1991) Reservoir fluid property correlations – state of the art. *SPE Reservoir Engineering*, **6**, 266–72.

Mercer JW, Pinder GF, Donalson IG (1975) A Galerkin-finite element analysis of the hydrothermal system at Wairakei, New Zealand. *Journal of Geophysical Research*, **80**, 2608–21.

Nield DA, Bejan A (1992) *Onset of Thermohaline Convection in Porous Media*. Springer-Verlag, New York.

Palliser C, McKibbin R (1998a) A model for deep geothermal brines, I: *T–P–X* state-space description. *Transport in Porous Media*, **33**, 65–80.

Palliser C, McKibbin R (1998b) A model for deep geothermal brines, II: Thermodynamic properties – density. *Transport in Porous Media*, **33**, 129–54.

Palliser C, McKibbin R (1998c) A model for deep geothermal brines III: Thermodynamic properties – enthalpy and viscosity. *Transport in Porous Media*, **33**, 155–71.

Person M, Garven G (1994) A sensitivity study of the driving forces on fluid flow during continental-rift basin evolution. *Geological Society of America Bulletin*, **106**, 461–75.

Phillips SL, Igbene A, Fair JA, Ozbek H, Tavana M (1981) *A Technical Databook for Geothermal Energy Utilization*. Lawrence Berkeley Laboratory Report 12810.

Person M, Neuzil C, Mailloux B, Wieck J, Toupin D, Bekele E, Eadington P, Garven G, Swenson J (1998) *RIFT*2D: A finite element model for simulating two-dimensional ground water flow, heat and solute mass transport within evolving basins. *Water Resources Investigations Report*.

Potter RWII, Brown DL (1917) The volumetric properties of sodium chloride solutions from 0 to 500 °C at pressures up to 2000 bars based on a regression of available data in literature. *US Geological Survey Bulletin*, **1421-C**.

Rowe AM, Chou JCS (1970) Pressure–volume–temperature–concentration relation of aqueous NaCl solutions. *Journal of Chemical Engineering Data*, **15**, 61–6.

Tremaine PR, Hill PG, Irish EE, Balakrishnan PV (eds) (2000) Release on the IAPWS Industrial Formulation 1997 for the thermodynamic properties of water and steam. In: *Proceedings of the 13th International Conference on the Properties of Water and Steam*, pp. A43–89. NRC Research Press, Ottawa.

Vand V (1948) Viscosity of solutions and suspensions. 2 Experimental determination of the viscosity concentration function of spherical suspensions. *Journal of Physical Chemistry*, **52**, 300–14.

Watson JTR, Basu RS, Sengers JV (1980) An improved representative equation for the dynamic viscosity of water substance. *Journal of Physical and Chemical Reference Data*, **9**, 1255–90.

Weast RC (ed.) (1988) *CRC Handbook of Chemistry and Physics*. CRC Press Inc, Boca Raton, FL.

Zarembo VI, Federov MK (1975) Density of sodium chloride solutions in the temperature range 25–350 °C at pressures up to 100 kg/cm^2. *Journal of Applied Chemistry USSR*, **48**, 2021–4.